SHADING-BASED TWO-VIEW MATCHING

Michel Audette, Paul Cohen and Juyang Weng
Department of Electrical and Computer Engineering
Ecole Poly technique
P.O.B. 6079 Station A
Montreal, Quebec, Canada, H3C 3A7
E-mail: cohen@ai.polymtl.ca

Abstract

This paper presents a region-based stereo matching algorithm, in which the regions are computed from the Gaussian *(K)* and mean *(H)* curvature information of the image intensity surface. A region is defined as a connected area of constant *K/H* sign combination, and thus constitutes the footprint of a local section of the intensity surface, whose shape is a peak, a pit, a positive or a negative saddle. Region adjacency information is explicited by means of a Voronoi graph representation of the region map. Matching between nodes of identical shape types in the two region maps is established by comparing the topological configuration of their immediate neighborhoods. The disparity map is established through a coarse-to-fine strategy.

1 Introduction

Computing 3-D structure from two stereoscopic or consecutive images requires the establishing of one-to-one correspondences between images primitives originating from the same elements of the scene. It is therefore essential to select, as primitives to be matched, image characteristics which strongly correlate with significant scene descriptors. Experiments with random stereograms, first introduced by Julesz [Jule60], have demonstrated that binocular matching does not necessitate a preliminary stage of high-level monocular recognition and can be based on local image primitives only. They have also shown that human stereopsis can tolerate substantial differences in intensity values and micropatterns between the two images. It is thus widely accepted that the correspondence problem cannot be efficiently solved by directly matching intensity values.

Techniques for solving the correspondence problem fall into two broad categories, namely the point-based and the region-based approaches. In the point-based category, Marr &: Poggio [MaPo79] proposed a theory of stereoscopic matching, using as primitives the zero-crossings of the image convolved with a Laplacian of Gaussian operator at different spatial resolutions. False niatchings are minimized by means of a coarse-to-fine matching strategy, in which the disparity range is progressively reduced while the resolution is progressively increased. Mayhew & Frishy [MaFrSl] later showed that zero-crossings alone cannot explain the perception of stereograms corresponding to saw-tooth intensity gratings and suggested using peaks of the intensity profile as additional matching primitives. Many other point-based matching algorithms were proposed. Some of them use correlation [GlRe83], some use edges [BaBi81; Grim85; OhKa85], others use segments [AyFa85], combinations of features [Weng89] or phase [jeJe89].

Region-based approaches involve extracting from the two images, areas which are uniform with respect to some image characteristics. Regions have been defined as areas of consistent grey-level intensity bounded by edges [LiBi87; CVSG89], of constant sign of the $\nabla^2 G \star I$ bandpass operator, of morphologically detected local peaks and valleys [FuMa89], or of black and white intensity produced by the projection of a filtered random dot pattern onto the scene [XuKT89].

Regional features possess certains advantages over points and lines. First, regions are more robust than edges because noise tends to perturb less a measurement taken over a region than one taken over its boundaries. This advantage was first noted by Nishihara [Nish83] who proposed a matching algorithm based on the regions delimited by the zero-crossings contours of V^2G*7. Second, the matching ambiguity problem should be less severe with regions because they give rise to a richer variety of features than points and segments. Third, occlusions have a more radical effect on points and lines than on two-dimensional primitives and should thus be less detrimental to the matching performance of a region-based matching algorithm. Finally, image descriptions in terms of regions implicitly contain region-adjacency information, which can be captured in a graph representation and constitute a powerful means of matching and disambiguation.

This paper presents a region-based matching algorithm, in which the regions are computed from the Gaussian *(K)* and mean (H) curvature information of the image intensity surface. A region is defined as a connected area of constant *K/H* sign combination, and thus constitutes the footprint of a local section of the intensity surface, whose shape is a peak, a pit, a positive or a negative saddle, depending on the particular *K/H* sign

combination [BeJa86]. Region adjacency information is explicited by means of a Voronoi neighborhood graph representation of the region map (or equivalently, the Delaunay triangulation) [PrSh88]. Each node is labelled with a feature vector which contains the shape type, the size and the mean intensity of the corresponding region, while the arc joining two adjacent nodes is labelled with the relative position of the corresponding regions. Matching, between nodes of identical shape types and similar average intensity, is established by comparing the topological configurations of their immediate neighborhoods. The disparity map is established through a coarse-to-fine strategy: regions are first extracted and matched at a coarser resolution in order to compute a rough estimate of the disparity map, which is then used to drive the matching procedure and the disparity computation at a finer level.

The use of Gaussian and mean curvature information to define the region primitives can be justified in several ways. First, since regions are areas of constant *K/H* sign combinations, their boundaries partially consist of the zero-crossings that would be used by an edge-based matching algorithm. However region boundaries are not limited to zero-crossings, and thus constitute a denser set of image elements. Second, the fact that *K/H* regions implicitly contain information about peaks of the intensity surfaces fits well with the argument that peaks of the intensity signal are useful primitives for stereopsis [MaFr8l]. Third, since Gaussian and mean curvatures constitute surface characteristics which remain invariant under a change of viewpoint, they should provide a stable description of the image intensity surface, in areas of quasi-Lambertian behavior.

Section 2 of this paper gives a brief outline of the complete matching algorithm, while sections 3 and *A* describe in more details the computation of the region map and the matching strategy respectively. Section 5 presents and discusses results obtained with real image pairs.

2 Algorithm Outline

The matching algorithm uses a coarse-to-fine strategy, which progressively increases the resolution and refines the disparity map estimation, using the local disparity obtained at a coarser level to drive the correspondence search at the next finer level. Each of the resolution stages consists of three different steps: (1) a region map extraction step, (2) a region matching step, and (3) a disparity map computation step.

The region map extraction step consists of all the processing operations required to select the proper level of resolution (Gaussian filtering), to compute the signs of the Gaussian and mean curvature of the intensity surface at each pixel location, to establish the modified Voronoi diagram of the curvature regions, and to label the nodes and the arcs of the diagram with the necessary intra-regional (shape type, size, mean intensity) and inter-regional (relative position) parameters respectively. The modified Voronoi diagram, together with the node and arc labels, constitute the region map.

The region matching procedure is applied to regions of the two images which are of the same shape type and of similar average intensities. It starts with an initial, possibly ambiguous, matching of regions based on a similarity measure of their neighborhood topology. In accordance with other multi-resolution strategies, the search for a match is conducted in a window, whose size is proportional to the current Gaussian parameter, centered at the local disparity value inherited from the coarser resolution level (a zero disparity value is assumed at the coarsest level). This first attempt may produce three types of results: a one-to-one match, an ambiguous (one-to-several) match, or a no-match result. For a one-to-one match, a disparity vector $(\Delta x, \Delta y)$ is computed. Ambiguous (one-to-several) matches are further treated by a recursive disambiguation procedure, which consists of choosing, among all the matching alternatives for a node, the one whose disparity best agrees with those of the currently validated (i.e. one-to-one) matches within the Voronoi neighborhood. An attempt is then made to reduce the amount of unmatched nodes, using a relaxed procedure (i.e. reduced search window and more tolerant dissimilarity test) which tries to find, for each such node, a one-to-one match around a disparity value in agreement with those of its Voronoi neighbors.

The disparity computation step consists of establishing, through interpolation, a dense disparity map at the current resolution stage. In order to prevent undesirable blurring across discontinuities, the interpolation procedure uses both the node disparity map established at the preceding step and an edge map obtained by means of a recursive edge detection operator [ShCa86].

The next two sections give details concerning the map extraction and the region matching steps.

3 Region Map Extraction

3.1 Computation of Gaussian and Mean Curvatures

Scale selection is accomplished by Gaussian filtering of the intensity values, i.e. by convolving the image intensity with the gaussian kernel:

$$G_\sigma(x,y) = \frac{1}{2\pi\sigma^2} exp[-\frac{x^2+y^2}{2\sigma^2}] \qquad (1)$$

The Gaussian (A) and the mean (H) curvatures are computed from the values of the first and second derivatives of the filtered intensity surface, according to the expressions:

$$K = \frac{f_{xx}f_{yy} - f_{xy}^2}{(1+f_x^2+f_y^2)^2} \qquad (2)$$

$$H = \frac{f_{xx} + f_{yy} + f_{xx}f_y^2 + f_{yy}f_x^2 - 2f_xf_yf_{xy}}{(1+f_x^2+f_y^2)^{3/2}} \qquad (3)$$

Computation of the derivatives requires a continuously differentiable intensity function. This can be accomplished by least-squares fitting a quadratic surface over a 5 x 5 neighborhood centered at each location. The derivatives needed to calculate *K* and *H* are then given by the coefficients of the basis functions obtained in performing the fit [BoCo84].

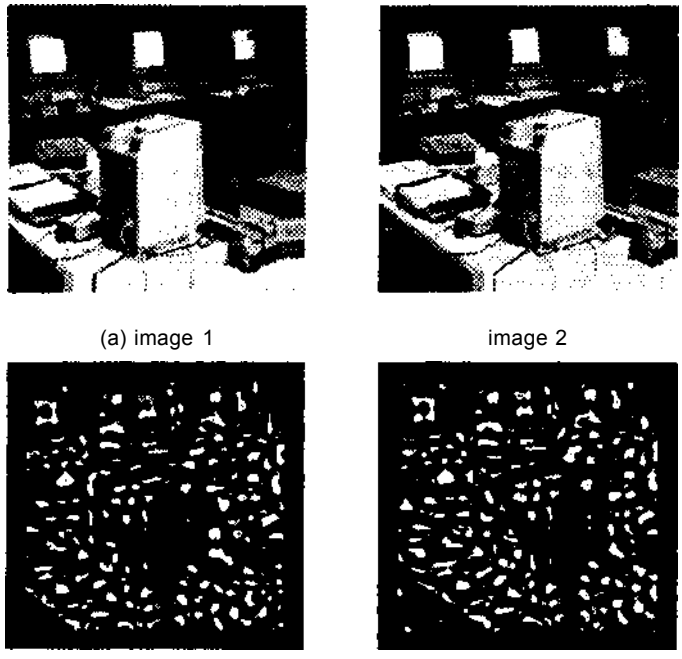

(a) image 1 image 2

(b) image 1 image 2

Figure 1: Region map extraction: (a) Original monocular pair; (b) Regions obtained at coarse resolution level ($\sigma = 8$). The four shape types are represented by four different grey-levels.

3.2 Definition of Curvature Regions

Regions of constant *K/ H* signs are then extracted by thresholding. Each region is the footprint of one among four possible shape primitives: a peak $(K > 0, H < 0)$, a pit $(K > 0, H > 0)$, a negative saddle $(K < 0, H < 0)$, and a positive saddle $(K < 0, H > 0)$. In fact, H and K values must be thresholded in order to confer to the region map some immunity to insignificant changes in curvature sign, caused by viewpoint changes in nearly flat areas of the intensity surface. In general, regions corresponding to positive or negative saddle shapes tend to be more elongated than those corresponding to peaks or pits. Since the later step of region matching will result in the association of a disparity value to a central location of each region (its centroid or maximum curvature location), it is desirable to keep all regions reasonably compact. Consequently, the thresholds on *K/H* must be selected so as to generate saddle regions whose compactness remains comparable to that of peaks and pits. Once properly detected, all the curvature regions R_n of each image are indexed by means of a component labelling routine. Figure 1 (a), (b) shows a temporal pair of images and the corresponding regions extracted at the coarsest level of resolution.

3.3 Definition of Regional Features

Four intra-regional features are associated with each region R_n: its shape type τ_n, its average intensity $\bar{I}_n$, its area S_n and the position (x_n, y_n) of its extremum of Gaussian curvature (called *region principal point* in the rest of the text). This last feature is not used during the matching procedure, but serves as anchor point of the region, in the computation of the local disparity. The location of curvature extremum is a better anchor point than the region centroid, because it tends to be less affected by changes of the region shape, induced by variations of the curvature threshold. A fifth regional feature, called the Neighborhood Matrix NM_n is defined in order to summarize information about the region immediate neighborhood. Its computation requires the transformation of the set of regions into a graph in which region adjacency is explicited. A natural choice for this graph is the modified Voronoi diagram [ToY088; PrSh88] of the curvature regions. Each node of the graph corresponds to a particular curvature region R_n and coincides with the location (x_n, y_n) of its principal point. It is labelled with the set of the four regional features $\tau_n, \bar{I}_n, S_n, NM_n$.

The aspects of the neighborhood information which are conveyed by the Neighborhood Matrix NM_n are the locations of Voronoi neighbors, as well as their own intraregional characteristics, namely their shape type, area and average intensity. This choice of characteristics is justified by the consistency of the relative position and orientation of each neighbor under changing viewpoint, as noticeable in the example of Figure 1. The area around the region under consideration is divided into 16 sectors and the neighbors are sorted according to the sector in which they fall. The matrix NM_n consists of 16 rows: the *kth* row enumerates the four characteristics of the closest neighbor whose principal point falls in the *kth* sector, namely

$NM_n(k,1)$: an integer (between 1 and 4) indicating the shape type of the neighbor,
$NM_n(k,2)$: its area,
$NM_n(k,3)$: its distance from the central region R_n,
$NM_n(k,4)$: its average intensity.

If no Voronoi neighbor falls into a sector, its corresponding row is empty.

4 Region Matching and Disparity Computation

4.1 Matching Criterion

The matching strategy consists of associating regions R_n and R_n' of the two images (i.e. nodes of the two region maps) which are of the same shape type and have highly similar neighborhoods:

$$match(R_n, R_{n'}) = true \quad if \begin{cases} & [\tau_n = \tau_{n'}] \\ .and. & [\epsilon_{nn'} = small] \\ .and. & [\gamma_{nn'} = small] \end{cases} \tag{4}$$

where $e_{nn}*$ is a measure of the dissimilarity between the two neighborhood matrices NM_n and $NM_{n'}$, and $y_{nn'}$ represents the absolute difference in average intensity between the two regions. Comparing the two neighborhood

matrices could consist of comparing each row of the first matrix to the corresponding row in the second one, which would amount to comparing Voronoi neighbors which fall in identical sectors in the left and right images. Such a comparison would be too strict however, since it would not allow any variation in neighborhood orientation under viewpoint change. In order to confer some flexibility to the comparison, the dissimilarity measure is defined as:

$$\varepsilon_{nn'} = \sum_{k=1}^{16} \varepsilon_{nn'}(k) \tag{5}$$

where

$$\varepsilon_{nn'}(k) = \min_{k'=k\oplus a,\ a\in\{-1,0,1\}} [1 - C\tau_{kk'}(\sigma_{kk'} + \delta_{kk'} + \gamma_{kk'})] \tag{6}$$

C is a normalizing constant and $\oplus$ designates modulo-16 addition operator. The min operator in expression (6) is used to allow a relative rotation of one sector in either direction, when comparing neighbors in the two region maps. $\varepsilon_{nn'}(k)$ is a penalty measure which takes into account differences in shape type, size, relative distance and mean intensity between the two neighbors under comparison. It uses threshold-type compatibility functions defined as follows:

- **Type Compatibility Function** $\tau_{kk'}$

$$\tau_{kk'} = \begin{cases} 1 & \text{if } NM_n(k,1) = NM_{n'}(k',1) \\ 0 & \text{otherwise} \end{cases} \tag{7}$$

Type compatibility is thus assumed if and only if the shape types of the two neighbors under consideration are identical.

- **Size Compatibility Function** $\sigma_{kk'}$

$$\sigma_{kk'} = \begin{cases} 1 & \text{if } \frac{|NM_n(k,2) - NM_{n'}(k',2)|}{NM_n(k,2) + NM_{n'}(k',2)} \le t_{area} \\ 0 & \text{otherwise} \end{cases} \tag{8}$$

where t_{area} is a relative area threshold (typically 30 %) which limits the acceptable size discrepancy between compatible neighbors.

Distance Compatibility Function $\delta_{kk'}$

$$\delta_{kk'} = \begin{cases} 1 & \text{if } |NM_n(k,3) - NM_{n'}(k',3)| \le t_{dist} \\ 0 & \text{otherwise} \end{cases} \tag{9}$$

where t_{dist} is an absolute threshold (typically 5 pixels) which limits the tolerable discrepancy of distance to the two central regions.

- Intensity Compatibility Function $\gamma_{kk'}$

$$\gamma_{kk'} = \begin{cases} 1 & \text{if } |NM_n(k,4) - NM_{n'}(k',4)| \le t_{int} \\ 0 & \text{otherwise} \end{cases} \tag{10}$$

where t_{int} is an absolute threshold (typically 8 grey levels, out of 256) which limits the tolerable discrepancy between average intensity of compatible neighbors.

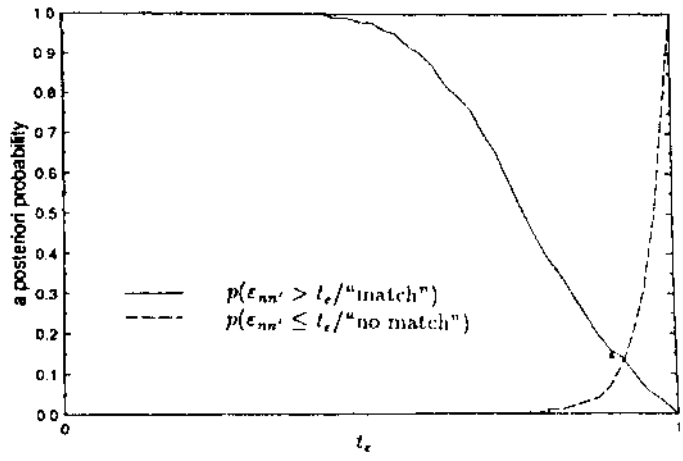

Figure 2: Statistical distributions of the dissimilarity measure under match and no-match assumptions

The ability of the dissimilarity measure $\varepsilon_{nn'}$ to correctly match regions of the two images is illustrated in Figure 2, which represents the statistical distributions of $\varepsilon_{nn'}$ for matching and unmatching regions. A discriminating threshold can be easily defined to minimize the probability of misclassification. The inclusion in the matching criterion (4) of a test on the average intensities of the central regions R_n and $R_{n'}$ aims at increasing the robustness to occlusion errors, which would otherwise occur if type and neighborhood alone were used.

4.2 Matching Procedure

As mentioned in section 2, a first step of the matching procedure consists of selecting, for each region (node) of the first image, all potential matching nodes in the second image within a search window whose size decreases with increasing resolution. Potential matches are selected on the basis of the dissimilarity measure $E_{nn'}$, using a decision threshold established by analysis of the distributions of Figure 2 (typically set to 0.80). At coarse resolution, a large search window (128-pixel wide for a 512x512 image) is used, since no a priori disparity information is available at this level. A square window is used in the case of temporal image pairs, while in the stereo case the epipolar constraint allows a reduction of the window height. Since matching is done between regions and not point features, the window cannot be reduced to one line segment but necessitates a height of a few pixels (typically 12), in order to allow for fluctuations in the position of the region principal points.

An efficient search strategy is an important consideration when matching discrete primitives. A bucketing technique is used to sort each region node according to the location of its principal point. The image plane is first divided into tiles, each of *4* x *4* pixels. A region whose principal point falls within a tile has its label stored in a memory location corresponding to this tile. The search window is centered at the tile which coincides with either the position of the region to be matched (at coarse resolution), or with this position offset by the cur-

t_{area}: t_{int}=7.5 t_{dist}=5.0	0.15	0.20	0.25	0.30	0.35	0.40
	277 / 3	277 / 3	280 / 3	283 / 3	285 / 4	285 / 4
t_{dist}: t_{int}=7.5 t_{area}=0.30	2.5	5.0	7.5	10.0	12.5	15.0
	277 / 3	283 / 3	289 / 6	291 / 6	291 / 6	298 / 6
t_{int}: t_{dist}=5.0 t_{area}=0.30	5.0	7.5	10.0	12.5	15.0	17.5
	267 / 2	283 / 3	296 / 11	298 / 11	301 / 15	305 / 11

Table 1: Matching score sensitivity to parameters variations (upper left: number of good matchings; lower right: number of false matchings; total number of regions: 481)

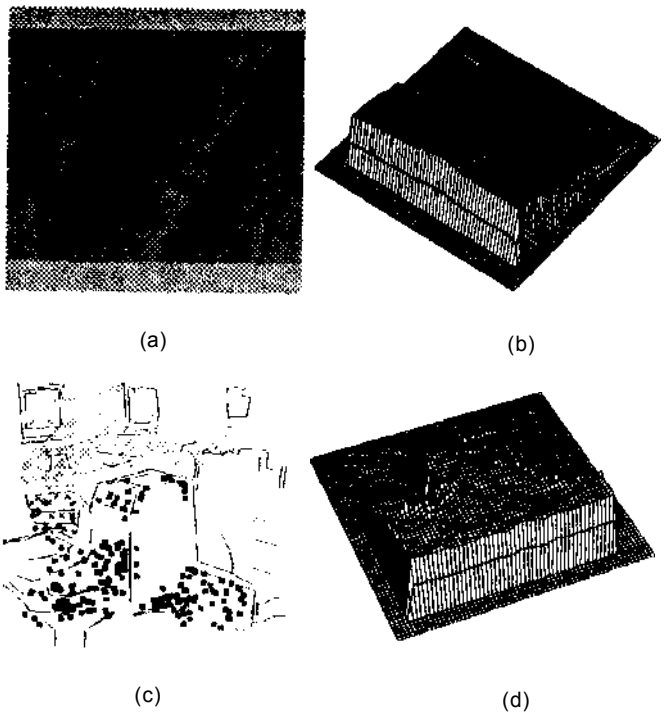

Figure 3: Disparity map: (a) original left image (stereo pair), (b) finer level ($\sigma = 4$) dense disparity map (stereo pair); (c) finer level ($\sigma = 4$) sparse disparity map, with edge map used to inhibit interpolation (temporal pair); (d) finer level dense disparity map (temporal pair)

rent disparity estimate (at higher resolutions).

In order to disambiguate between multiple potential matches, a disparity continuity constraint is applied, using neighboring information within an iterative procedure. For each region, a disparity estimate is established using the median of the disparity values of the currently validated neighboring matches. Taking the median of x- and y-components of the disparity values rather than their mean provides some immunity to outliers. Comparing then the disparity estimate with all corresponding potential matches allows us to select the match whose actual disparity is the closest to the estimate. This disambiguation step is allowed to iterate until there is no change in the number of validated matches.

The disparity continuity constraint is also used to force additional matches at the same resolution. For each unmatched region, a disparity estimate is established by taking a weighted average of the disparity values of the validated neighbors. Each weight is inversely proportional the distance ($NM_n(k,3)$) and is normalized so that all weights sum to 1. The search window is centered on the tile corresponding to the principal point position offset by this new estimate, the window size radius is reduced, and the dissimilarity threshold is increased.

5 Results and Discussion

Table 1 illustrates the performance of the matching procedure, in the case of the temporal image pair of Figure 1, under variations of the dissimilarity measure parameters, and shows that the choice of such parameters does not critically affect the performance of the algorithm.

Figure 3 illustrates the kind of results obtained with a stereo pair and with the temporal pair of Figure 1, at a finer resolution level ($\sigma = 4$). The left original stereo image is featured in (a), and its corresponding disparity map is plotted in (b). To demonstrate the density of the results extracted at this scale, a sparse density map for the temporal pair is shown in Figure 3 (c), where intensity is inversely proportional to the disparity value and thus proportional to range. The edge map used to inhibit interpolation is also shown in Figure 3 (c). Finally, Figure 3 (d) features a plot of the dense disparity map, for the temporal pair. The disparity values extracted for every region at the coarsest resolution are used to drive the matching at the finer one.

The interpolation scheme used here is based on Sinha & Schunck's method [SiSc89; SiSc90], which uses a least-median-squares approximation stage followed by a weighted bicubic spline interpolation stage. The approximation performs a fit at each point defined on a regular grid, using nearby (irregularly spaced) sparse disparity data. This fitting provides regularly spaced disparity values, which are necessary for a spline-based surface interpolation.

We modify the approximation stage as follows: we discount any disparity value defined at a point which lies across a discontinuity from the point where we are performing the fit. The motivation for this modification to the approximation scheme is that least-median-squares fitting provides noise immunity by ignoring outliers in the disparity data, but near discontinuities the number of outliers approaches the number of disparity values over

which it is desirable to perform the fit. The fitting step yields a value consistent with the majority of neighboring points, and this would produce an incorrect disparity estimate if this value were dictated by undesirable points (e.g.: points lying outside of the boundary of an object over which we are fitting), if they were not eliminated.

6 Conclusion

This paper has described a region-based stereo matching algorithm, in which the regions are defined as areas of the intensity surface having constant-sign Gaussian *(K)* and mean (H) curvatures. Region adjacency information is explicited by means of a Voronoi graph representation of the region map. Matching between nodes of identical shape type in the two region maps is established by comparing the topological configuration of their immediate neighborhoods. The disparity map is established through a coarse-to-fine strategy. All operations concerning region map extraction and regional feature calculation involve simple local computations, and make the algorithm suitable for efficient parallel implementation. Results presented indicate that the algorithm is reliable and produces dense disparity maps. Further experiments are under way in order to assess the performance in a wide range of situations.

7 Acknowledgement

This work has been supported by the Institute for Robotics and Intelligent Systems (IRIS) under the Canadian program of Networks of Centres of Excellence. The help of Nguyen Hong Hai, computer analyst in our group, concerning various aspects of the algorithm implementation is gratefully acknowledged.

References

[AyFa85] N. Ay ache &. B. Faverjon, Fast stereo matching of edge segments using prediction and verification of hypotheses, *Proc. CVPR,* San Francisco, Ca., 1985.

[BaBi8l] H.H. Baker *k* T.O. Binford, Depth from edges and intensity based stereo, *Proc. 1JCA1,* Vancouver, B.C., 1981.

[Bc.7a86] P.J . Besl & R.C. Jain, Invariant surface characteristics for 3D object recognition in range images, *CVGIP 33,* 1986.

[BoCo84] R.M. Bolle & D.B. Cooper, Bayesian recognition of local 3-D shape by approximating image intensity functions with quadric polynomials, *IEEE Trans. PA* MA/, Vol. 6, 1984.

[CVSG89] L. Cohen, L. Vinet, P.T. Sander, & A. Gagalowicz, Hierarchical region based stereo matching, *Proc. CVPR,* Washington, D C , 1989.

[FuMa89] C.S. Fuh & P. Maragos, Region-based optical flow estimation, *Proc. CVPR,* Washington, D C , 1989.

[GlRe83] , F. Glazer, *G.* Reynolds, and P. Anandan, Scene matching by hierarchical correlation, *Proc. CVPR,* 1983.

[Grim85] W.E.L. Crimson, Computational experiments with a feature based stereo algorithm, *IEEE Trans. PA MI,* vol. 7, 1985.

[JeJe89] A D . Jepson, M.R.M Jenkin, The fast computation of disparity from phase differences, *Proc. CVPR,* San Diego, Ca., 1989.

[Jule60] B. Julesz, Binocular depth perception of computer-generated patterns, *Bell Syst. Tech. J.,* Vol. 39, 1960.

[LiBi87] U.S. Lim & T.O. Binford, Stereo correspondence: a hierarchical approach, *Proc. Image Unders. Workshop,* Los Angeles, Ca., 1987.

[MaPo79] D. Marr *k* T. Poggio, A computational theory of human stereo vision, *Proc. Roy. Soc. London,* B, Vol. 204, 1979.

[MaFr8l] J.E.W Mayhew *k* J.P. Frisby, Psychophysical and computational studies towards a theory of human stereopsis, *Artif. Intell,* Vol. 17, 1981.

[MeMR90] P. Meer, D. Mintz *k* A. Rosenfeld, Robust Recovery of Piecewise Polynomial Image Structure, *Proc. Workshop on Robust Computer Vision,* 1990.

[Nish83] H.K. Nishihara, Practical real-time imaging stereo matcher, *Optic. Enginr.,* Vol. 23, 1984.

[OhKa85] Y Ohta & T. Kanade, St ereo by Intra- and Inter-Scanline Search Using Dynamic Programming, *IEEE Trans.* /MM/, vol. 7, 1985.

[PrSh.88] F.P. Preparata & M.I. Shamos, *Computational Geometry, an Introduction,* Springer-Verlag, 1988.

[ShCa86] J. Shen *k* S. Castan, An optimval linear operator for edge detection, *Proc. CVPR,* 1986.

fSiSc89] S.S. Sinha & B.G. Schunck, Discontinuity preserving surface reconstruction, *Proc CVPR,* 1989.

[SiSc90] S.S. Sinha & B.C. Schunck, A robust method for surface reconstruction, *Proc. Workshop on Robust Computer Vision,* 1990.

[T0Y088] F.I. Toriwaki & S. Yokoi, Voronoi and related neighbors on digitized two-dimensional space with applications to texture analysis, *Computational Morphology,* North-Holland, 1988.

[Weng89] J. Weng,N. Ahuja, and T. Huang,Two-view matching, *Proc. ICCV,* Tampa, FI, 1988.

[XuKT89] G. Xu, H. Kondo, *k* S. Tsuji, A region-based stereo algorithm, *Proc. IJCAI,* 1989.